

Gaussian-Based Smoothing of Wind and Solar Power Productions Using Batteries

Alemayehu A. Desta, Pierre Courbin, and Vincent Sciandra
METRON, Paris, France

Email: alemayehu.addisu@metronlab.com, {pierre.courbin, vincent.sciandra}@metronlab.com

Laurent George
UPEM and ESIEE, Champs-sur-Marne, France
Email: laurent.george@esiee.fr

Abstract—Intermittent nature of Distributed Energy Resources (DER) such as solar and wind cause significant power fluctuations and integrating them to a power systems requires control mechanisms to reduce fluctuations. One way to control the effect of fluctuation is to use Energy Storage Systems (ESS) for smoothing out their power productions. A typical method to attain this goal is to use ESS with classical moving average approaches. However, these methods are affected by peaks and troughs in power production due to cloud passing and wind gust effects on solar panels and wind turbines, respectively. In this paper, we propose a Gaussian-based smoothing method to alleviate pitfalls of moving average methods to smooth out forecasted values of solar and wind powers. Then, we determine a minimum ESS size required to maintain a smoothed power curve for a day-ahead period. From our experiments, the proposed algorithm requires smaller ESS size than the classical approaches.

Index Terms—distributed energy resources, solar, wind, moving average, gaussian-based, microgrid

I. INTRODUCTION

Developing clean energy through integration of Distributed Energy Resources (DERs) and insuring energy safety have gained much attention from energy industry. However, integration and control of DERs pose challenges to management and operation of power systems such as microgrid [1]. For instance, solar output power changes frequently depending on the position of the sun and clouds. Wind output power is also subject to some of the same types of daily and seasonal variations in wind speeds. These fluctuations in power generation require different approaches to smoothly integrate the DERs to microgrids. A potential candidate solution to these challenges is using ESS such as Battery Energy Storage Systems (BESS) [2] [3], electric double-layer capacitor [4], superconducting magnetic energy storage [5], and fuel cells [6]. The ESS can be used to store surplus energy when energy production is higher than energy demand and to shave peak demands. Furthermore, it can be used to fill voids created by forecasting errors.

For smoothing out fluctuating power generation of wind and solar, different approaches have been proposed in literatures. A Moving Average (MA) method was proposed in [7] and [8]. They deployed the MA method to reduce short-term fluctuation of photovoltaic (PV) power using batteries. Furthermore, the MA approach was also used in [3] for controlling battery energy to reduce PV power fluctuation. In [9], an Exponential Moving Average (EMA) with hydrogen storage system was used. The difference between MA and EMA is that the EMA gives more weights on recent values of a fluctuating variable. In both MA and EMA, length of an averaging window determines how storage systems charge or discharge. If the averaging window is long, the storage system is required charge or discharge more than needed even if the fluctuation is not significant [10]. Another approach was proposed in [11]. It is based on a fuzzy wavelet transform method to smooth out wind and solar power productions using ESS.

In this paper, we propose a Gaussian-based method for smoothing out fluctuation of wind and solar powers using BESS. We compare the performances of the proposed algorithm against MA and EMA approaches based on actual and forecast datasets for industrial site located in France. Then, we determine a minimum battery size in order to guarantee a power production curve for a day-ahead period. Our goal is to determine such a power curve with minimum battery size. Knowing beforehand the precise power generation can help one to make decisions on when and how much energy to buy either from a main grid or spot markets if demand is higher than supply.

The remainder of this paper is organized as follows. In Section II, we discuss few notations and models of DERs. Then, in Section III, we detail the smoothing algorithms and our problem formulation. We provide our experimental results and discussions in Section IV. Finally, in Section V, concluding remarks are provided.

II. NOTATIONS AND MODELS

In this section, we provide models and notations of solar, wind, storage systems, and spot market.

A. Solar Power

Solar panels convert energy from the sun into electrical energy in a PV system. Solar panels are composed of a number of solar cells that contain semiconducting materials which exhibit photovoltaic effects.

In a PV system, the electricity generated by a solar cell can be given as [12]:

$$P_{pv}(t) = GHI(t) * S * \eta \quad (1)$$

where GHI is global horizontal irradiation (W/m^2), S is surface area (m^2), and η is conversion efficiency of a solar panel. According to MacKay [13], typical solar panels have efficiency of about 10%; expensive ones with tracking device can perform up to 20%. Recently, a solar panel with 22.8% efficiency is reported by SunPower.

B. Wind Power

Wind turbines use rotors and blades to generate electrical power by extracting kinetic energy from air flow. Power generation could be of significant amount if the turbines are installed in locations with strong and sustainable wind speeds such as offshore areas.

A typical wind turbine is characterized by its power curve [14]. The curve shows the power extracted from wind speed. The following equation gives a relationship between extracted powers from corresponding wind speed:

$$P_w = (\rho/2) * A_{wt} * c_p(\lambda, \theta) * v_w^3 \quad (2)$$

where P_w is power extracted from wind (W), ρ is air density (kg/m^3), c_p is power coefficient of wind turbine, λ is ratio of v_t/v_w (ratio between blade tip speed (m/s) and wind speed at hub height upstream the rotor (m/s)), θ is pitch angle, and A_{wt} is area covered by wind turbine blades (m^2). Betz's limit [15] puts the maximum power coefficient limit to 59.3%. No wind turbine can extract kinetic energy from wind speed higher than this coefficient. In the simulation section, we put c_p to 25% as this value is commonly used.

C. Storage

TABLE I. CHARACTERISTICS OF COMMON BATTERY TYPES

Characteristics	Battery types	
	Lead-acid	Lithium-ion
Efficiency	0.75	0.85
Depth of Discharge	0.8	0.8
Self-discharge per day (%)	0.3	0.1
Energy density (Wh/L)	80	150
Power density (W/L)	125	450
Life cycle	2000	5000
Expected lifetime (Years)	4	10

Common storage technologies in use today include mechanical, thermodynamic, electrochemical and electromagnetic [16]. Among electrochemical storage

devices, most common battery types are lead-acid and lithium-ion batteries. These devices are an integral part of microgrids which allow smoothing of renewable energy resources and time-shifting of energy demands from peak hours.

Some characteristics of the two battery types such as Depth of Discharge (DoD), energy and power densities, efficiency and other features are shown in Table I [16].

Charging and discharging processes of a battery is described as [17]:

$$b(t+1) = \begin{cases} b(t) + \Delta t * P^c(t) & \text{charging} \\ b(t) - \Delta t * P^d(t) & \text{discharging} \end{cases} \quad (3)$$

where $b(t)$ represents state of battery at time t , Δt is time step, and $P^c(t)$ and $P^d(t)$ are charging and discharging power rates, respectively.

For normal operations of a battery, different constraints are imposed on power and energy limits. For example, stored energy cannot be greater than its predefined capacity (C) and cannot be lower than its minimum size (C_{min}), that is,

$$C_{min} \leq b(t) \leq C \quad (4)$$

There are also constraints on charging and discharging power rates, that is,

$$0 \leq P^c(t) \leq P^c_{max}(t) \quad (5)$$

$$0 \leq P^d(t) \leq P^d_{max}(t) \quad (6)$$

where $P^c_{max}(t)$ and $P^d_{max}(t)$ represent maximum charging and discharging rate limits at time t .

D. Spot Market

It is a market where electricity can be sold and purchased with different rates for different hours of the day. There exist two spot market types: day-ahead and real-time markets. In day-ahead spot markets, energy prices are announced to buyers and sellers a day ahead (around noon). For real-time markets, the sellers and buyers perform energy transaction close to real-time (in interval of 15 minutes). In Europe, European Power Exchange (EPEX) functions as a marketplace for day-ahead spot markets. It operates in France, Germany, Austria, and Switzerland. The EPEX determines spot market selling and buying prices based on intersection of demand and offer curves.

In EPEX spot market, the minimum energy for buyers and sellers is 1MWh. Therefore, based on the performances of the smoothing algorithms, we can determine the exact amount of energy to buy either from the main grid or the sport markets.

In the next section, we formulate our problem and setup mathematical formulations for the proposed algorithm along with the classical smoothing algorithms.

III. PROBLEM FORMULATION

In the above section, we provided few notations and models of solar, wind, storage and spot markets. In this section, we first analyze the smoothing algorithms for a solar, wind and battery hybrid system. Then, we

determine a battery size so that a smoothed production curve will be maintained for a day-ahead forecast period.

A. Solar/Wind Power Smoothing

Fig. 1 shows a conceptual schema of a hybrid system consisting of solar, wind and battery. Based on the figure, we first sum solar and wind powers that are forecasted for a day-ahead period. Then, we apply the proposed smoothing algorithm to smooth out power fluctuations. After that, the battery will be charged or discharged based on the output of the algorithms in order to make-up the difference between the actual and the smoothed forecast. We describe the proposed algorithm together with the moving average in the following section.

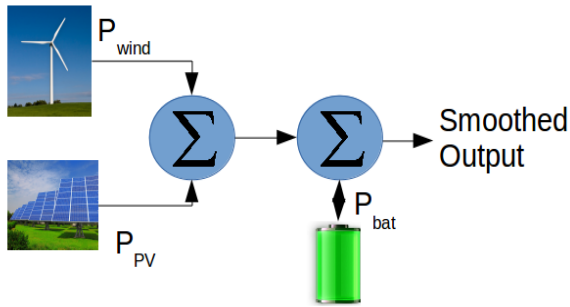


Figure 1. A conceptual schematic representation of solar, wind and battery hybrid system.

B. The Proposed Algorithm vs. Moving Average

1) *Moving average based smoothing:* A moving average approach was used in [7] and [8] to control energy storage device. According to [18], a moving average is a well know low-pass filter for time series data and it is formulated as:

$$y_w(i) = (1/w) \sum_{k=0}^{w-1} y(i-k), 0 \leq k \leq w-1 \quad (7)$$

where $y(i)$ is a time series data with a window length of w . Exponential moving average is an extension of simple moving average by giving more weights to recent values [9].

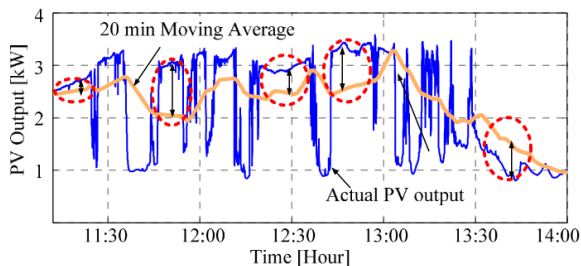


Figure 2. A 20 minute moving average of an actual PV output [10]

Although it is a classical way to reduce fluctuations in renewable resources, it exhibits a memory effect that generally depends on the window length w . A moving average with window length w contains $(1/w)$ % of present values. Fig. 2 shows the memory effect with window size of 20 minutes on a real PV power data as described in [10]. From the figure, we can see that the moving average values in broken circles deviate significantly from the actual PV power due to memory

effect of the moving average. However, the fluctuation in real PV Power is small in these periods. Hence, to accommodate the difference, the battery has to be charged or charged more than needed. To mitigate this problem, we propose a Gaussian-based method.

2) *Gaussian-based smoothing:* The Gaussian filter has been a de-facto standard for applications such as image processing and computer vision. A Gaussian function for one dimensional data is [19]:

$$G(x, \sigma) = (1/\sqrt{2\pi\sigma}) \exp^{-x^2/(2\sigma^2)} \quad (8)$$

where σ is the standard deviation of a Gaussian distribution and x is one dimensional input data. Typically, σ is used as a smoothing parameter in Gaussian-based method. Therefore, we use σ as smoothing parameter and change its values in order to see its effects on smoothing.

An application of the Gaussian filter is described in [28] for suppressing impulse noises. In our context, the noises represent power glitches due to cloud passing over PV panels and wind gust effects. Mitigating the peaks and troughs will result in smooth power generation from renewable energy resources.

After smoothing power fluctuations using the proposed algorithm, the next step is to determine battery size by considering the difference between the actual and the smoothed forecast one.

C. Determining Battery Size

We determine battery size C (in kWh) based on power difference between the actual and the smoothed one. For a discharging case, that is, when the actual power $P_{act}()$ is less than the smoothed power $P_{sm}()$, discharge energy can be calculated as:

$$E_d = \int [P_{sm}(t) - P_{act}(t)] dt, 0 \leq t \leq T \quad (9)$$

where T has interval of 1 hour. Then, for charging case:

$$E_c = \int [P_{act}(t) - P_{sm}(t)] dt, 0 \leq t \leq T \quad (10)$$

Finally, the rated capacity C is:

$$C = \max(E_d, E_c) \quad (11)$$

Eq. (11), which is similar to an equation defined in [2], considers charging and discharging cycles separately to determine battery size. However, in reality, a battery alternates between charging and discharging multiple times during operations. This results in a smaller battery size. To do this, we consider consecutive charging and discharging cycles. For example, we set up a recursive function for a discharging case as in:

$$E(t+1) = \begin{cases} E(t) + P_{sm}(t) - P_{act}(t) & \text{if discharging} \\ 0 & \text{otherwise.} \end{cases} \quad (12)$$

$$E_d = \max(E) \quad (13)$$

Eq. (13) takes the maximum of consecutive sums for discharging case. For charging case, the same kind of equation can be setup easily. Finally, the battery size C is determined by taking the maximum of the two cases. In

our simulation section, the results of these equations are shown.

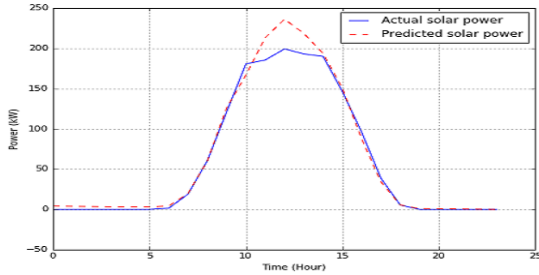


Figure 3. Real and predicted solar power for 24 hours

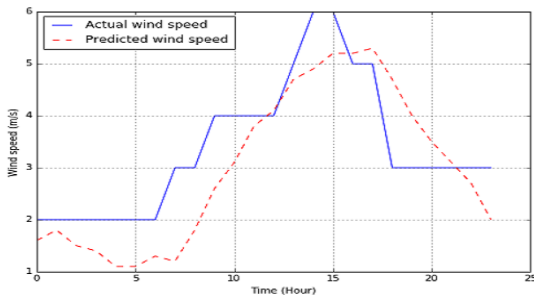


Figure 4. Real and predicted wind speed for 24 hours

IV. SIMULATIONS

In this section, we provide descriptions of our solar and wind datasets and discussions on obtained results.

A. Description of Datasets

For our simulations, we consider real solar and wind datasets for an industrial site located in Bourbourg, France. The datasets contain the following data.

1) *Solar data*: we retrieved hourly per unit (25m²) solar PV data from PVWatts[20] of National Renewable Energy Laboratory(NREL). We take power production of 100 units of PV panels for our simulation. Then, we use Auto Regressive Integrated Moving Average (ARIMA) model [21] to forecast day-ahead solar power production. Forecast and real solar data are shown in Fig. 3.

2) *Wind speed data*: hourly average wind speed for 2014 was obtained from *Weather Underground* website [22]. We use eq. (2) to compute the power extracted from given wind speed for a 3MW wind turbine [23]. Then, we apply ARIMA for a day-ahead forecast. Fig. 4 shows the real and predicted wind speed on September 17, 2014.

B. Results and Discussions

In this section, we compare the performances of the smoothing algorithms by varying smoothing parameters. Then, based on the results, we determine a minimum battery size so that a power production curve can be guaranteed for a day-ahead period.

1) *Performance of the smoothing algorithms*: in our work, we use standard deviation (σ) and averaging window (w) as smoothing parameters for Gaussian-based and window-based algorithms, respectively. We first set σ to 1 and w to 3. Fig. 5 shows the results of the three smoothing algorithms for the given σ and w . From the

figure, we can see that the Gaussian-based coincides with predicted power than Simple Moving Average (SMA) and Exponential Moving Average (EMA) methods. To see the effects of increasing smoothing parameters, we consider Fig. 6. In this case, we set σ to 2 and w to 5. For this case, the curve of Gaussian-based is more flat and the curves of SMA and EMA are more shifted to the right. The increase of smoothing parameters increase charge or discharge rates. For example, when σ is 1 and w is 3, the charging rates are 154, 156, and 162kW for Gaussian-based, SMA and EMA, respectively. However, when σ is 2 and w is 5, charging rates increase to 188, 200, and 221kW, respectively. This gives rise to a bigger battery size. Hence, the choice of the parameters enables one to make a compromise between more smooth power and battery size.

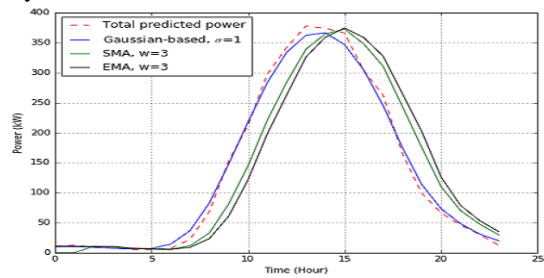


Figure 5. Smoothing forecast data when $\sigma=1$ and $w=3$

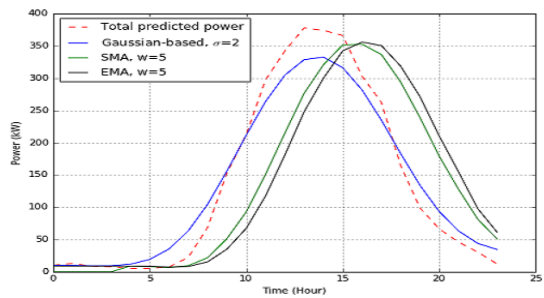


Figure 6. Smoothing forecast data when $\sigma=2$ and $w=5$

TABLE II. BATTERY SIZES FOR DIFFERENT PARAMETERS

Capacity (kWh)	Algorithms					
	Gaussian-based		SMA		EMA	
	$\sigma=1$	$\sigma=2$	$w=3$	$w=5$	$w=3$	$w=5$
E_c	308	412	820	1199	914	1337
E_d	271	310	575	890	681	1049
$C = \max(E_c, E_d)$	308	412	820	1199	914	1337

2) *Sizing of battery*: we can determine battery size by taking the difference between the actual power and the smoothed forecast one. A positive difference shows a charging case and a negative difference shows otherwise. In our experiment, we varied the smoothing parameters and then determine the corresponding battery size. Table II shows the results of our simulations for battery sizing using eq. (12) and (13). From the table, the Gaussian-based method required 62% less battery size than SMA and 66% less battery size than EMA when σ is 1 and w is

3. If we increase the parameters, the Gaussian-based method also outperforms the other two. However, there is an increase in battery size as we increase the parameters (See Table II).

3) *Power production curve*: the final output of our experiments is a power production curve for a day-ahead period. To attain this goal, we performed simulations to determine a smoothing algorithm that results in minimum battery size. As the results show, the proposed algorithm requires minimum battery size to smooth out power fluctuations in PV and wind. Fig. 7 shows the power production curve determined by using the Gaussian-based when σ is 1 as it gives the minimum battery size of 308kWh. If we use eq. (11) to determine battery size, it will be 536kWh. Hence, we gained a reduction of 128kWh by considering inter charge and discharge cycles rather than considering the cycles separately.

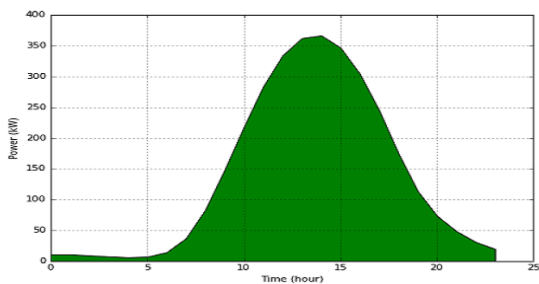


Figure 7. A power production for day-ahead period

V. CONCLUSIONS

In this paper, we proposed a Gaussian-based smoothing algorithm and compared its performance with classical smoothing algorithms such as Simple Moving Average (SMA) and Exponential Moving Average (EMA) to smooth out fluctuations in PV and wind power generations. To compare their performances, we used real datasets for an industrial site in France. From our simulations, the proposed algorithm has required at least 62% less battery size than SMA and EMA. In our work, we considered a one day-ahead forecast and we assumed perfect battery properties and no energy losses during conversion. As a future work, we would like to address these issues to match real life case.

REFERENCES

[1] R. H. Lasseter and P. Paigi, "Microgrid: A conceptual solution," in *Proc. IEEE 35th Annual Power Electronics Specialists Conference*, vol. 6, 2004, pp. 4285-4290.

[2] S. Chen, H. B. Gooi, and M. Wang, "Sizing of energy storage for microgrids," *IEEE Transactions on Smart Grid*, vol. 3, no. 1, pp. 142-151, 2012.

[3] T. D. Hund, S. Gonzalez, and K. Barretti, "Grid-tied pv system energy smoothing," in *Proc. 35th IEEE Photovoltaic Specialists Conference*, 2010, pp. 002762-002766.

[4] N. Nakimoto, H. Satoh, S. Takayama, and K. Nakamura, "Ramp-rate control of photovoltaic generator with electric double-layer capacitor," *IEEE Transactions on Energy Conversion*, vol. 24, no. 2, pp. 465-473, 2009.

[5] K. S. Tam, P. Kumar, and M. Foreman, "Enhancing the utilization of photovoltaic power generation by superconductive magnetic energy storage," *IEEE Transactions on Energy Conversion*, vol. 4, no. 3, pp. 314-321, 1989.

[6] S. Rahman and K. S. Tam, "A feasibility study of photovoltaic-fuel cell hybrid energy system," *IEEE Transactions on Energy Conversion*, vol. 3, no. 1, pp. 50-55, 1988.

[7] A. Ellis, D. Schoenwald, D. Hawkings, and S. Willard, "Pv output smoothing with energy storage," in *Proc. 38th IEEE Photovoltaic Specialists Conference*, 2012, pp. 001523-001528.

[8] J. Johnson, A. Ellis, A. Denda, K. Morino, T. Shinji, T. Ogata, and M. Tadokoro, "Pv output smoothing using a battery and gas engine-generator," in *Proc. 39th IEEE Photovoltaic Specialists Conference*, 2013, pp. 1811-1816.

[9] S. G. Tesfahunegn, O. Ulleberg, P. J. Vie, and T. M. Undeland, "Pv fluctuation balancing using hydrogen storage – a smoothing method for integration of pv generation into the utility grid," *Energy Procedia*, vol. 12, pp. 1015-1022, 2011.

[10] M. Alam, K. M. Muttaqi, and D. Sutanto, "A novel approach for ramp-rate control of solar pv using energy storage to mitigate output fluctuations caused by cloud passing," *IEEE Transactions on Energy Conversion*, vol. 29, no. 2, 2014.

[11] X. Li, Y. Li, X. Han, and D. Hui, "Application of fuzzy wavelet transform to smooth wind/pv hybrid power system output with battery energy storage system," *Energy Procedia*, vol. 12, 2011.

[12] Y. Ru, J. Kleissl, and S. Martinez, "Storage size determination of grid-connected photovoltaic systems," *IEEE Transactions on Sustainable Energy*, vol. 4, no. 1, 2013.

[13] D. MacKay, *Sustainable Energy—Without the Hot Air*, UIT Cambridge, 2008.

[14] C. Carrillo, A. O. Montano, J. Cidras, and E. Diaz-Dorado, "Review of power curve modelling for wind turbines," *Renewable and Sustainable Energy Reviews*, vol. 21, pp. 572-581, 2013.

[15] V. L. Okulov and J. N. Sorensen, "Refined betz limit for rotors with a finite number of blades," *Wind Energy*, vol. 11, no. 4, 2008.

[16] H. Chen, T. N. Cong, W. Yang, C. Tan, Y. Li, and Y. Ding, "Progress in electrical energy storage system: A critical review," *Progress in Natural Science*, vol. 19, no. 3, 2009.

[17] S. Chen, H. B. Gooi, and M. Wang, "Sizing of energy storage for microgrids," *IEEE Transactions on Smart Grid*, vol. 3, no. 1, 2012.

[18] E. Alessio, A. Carbone, G. Castelli, and V. Frappietro, "Second-order moving average and scaling of stochastic time series," *The European Physical Journal B-Condensed Matter and Complex Systems*, vol. 27, no. 2, 2002.

[19] S. M. M. Roomi, I. Lakshmi, and V. A. Kumar, "A recursive gaussian weighted filter for impulse noise removal," *GVIP Journal*, vol. 6, no. 3, 2006.

[20] PVWatts. [Online]. Available: <http://pvwatts.nrel.gov/>

[21] J. D. Hamilton, *Time Series Analysis*, Princeton University Press, vol. 2, 1994.

[22] Weather Underground. [Online]. Available: <https://french.wunderground.com>

[23] Vestas V112-3.0MW wind Turbine. [Online]. Available: www.vestas.com/en/products/turbines/v112-3_3_mw



Alemayehu A. Desta was born in Ethiopia. He received his BSc degree in Electrical and Computer Engineering (Computer Stream) from Addis Ababa University, Addis Ababa, Ethiopia in 2007. Then, he earned his MSC degree in Computer and Communication Networks Engineering from Polytechnic University of Turin, Turin, Italy in 2013. Currently, he is a PhD student in METRON SAS, Paris, France and University Paris-Est Marne-la-Vallée (UPEM), Champs-sur-Marne, France. His research interests are smart grid, microgrid, demand response, and real-time scheduling.



Laurent George was born in France. He completed his PhD degree at INRIA Paris, France in 1998. Currently, he is a professor at ESIEE Paris, member of LIGM lab at University Paris-Est Marne-la-Vallée (UPEM) and associate researcher at INRIA Paris-Rocquencourt in the AOSTE team. He received the habilitation to direct research in 2008 on the subject: "Temporal robustness for embedded and distributed real-time

systems". He is delegate at INRIA/AOSTE (Rocquencourt, France) team since September 2009.

Prof. Laurent George's research activities focus on feasibility conditions for hard real-time embedded and distributed systems (wired and wireless networks). He co-founded in October 2010 the ACTRISS group, supported by GDR ASR (CNRS, France), to federate and promote research in real-time systems in France. He is involved in many research projects on real-time systems with the automotive and the aerospace industry.



Pierre Courbin was born in France. In 2013, he completed a PhD degree in Computer Science (Parallel computing and Real-Time Scheduling for multiprocessors systems) at University Paris-Est Marne-la-Vallée (UPEM). In 2009, he obtained his Master2 degree from the University Paris-Sud 11, Orsay, and his degree of engineering from ECE Paris Engineering School specialized in "embedded systems".

Between 2004 and 2016, he created and headed a research/teaching department at ESILV Paris-La Défense engineering school specialized on digital and energy management. He is now CTO of METRON SAS, Paris, France.

Dr. Pierre Courbin's research interests are smart grid, microgrid, demand response and real-time scheduling for energy optimization.



Vincent Sciandra completed a PhD degree at University Paris-Est Marne-la-Vallée (UPEM) in Computer Science (Intelligent Transportation Systems) in 2013. He finished his engineering degree in "embedded systems" at ECE Paris Engineering School in 2007. Currently, he is a CEO of METRON SAS, Paris, France.

He is also a co-founder of METRON SAS.

Dr. Vincent Sciandra's research interests are smart grid, microgrid, demand response and real-time scheduling for energy optimization.